CHARACTERIZATION OF THE UNDULATOR MAGNETIC FIELD QUALITY BY THE ANGLE AVERAGED RADIATION SPECTRUM*

O. A. Shevchenko#, Budker INP SB RAS, Novosibirsk, Russia
N. Vinokurov, Budker INP SB RAS, Novosibirsk, Russia, and KAERI, Daejon, Rep. of Korea

Abstract

The real undulator magnetic field always contains errors which influence undulator performance. The effect of these errors is usually characterized by broadening of the spontaneous emission spectrum at zero angle and corresponding reduction of the spectral intensity. This approach works very well for the phase errors while it does not take into account transversal trajectory displacements. The integrated over the angles radiation spectrum contains more complete information about the undulator field quality but its calculation requires more effort. Therefore the spectral density of emitted radiation (the total number of emitted photons with given energy) can be considered as a figure of merit for an undulator. In this paper we derive analytical formula for this spectrum suitable for doing efficient numerical calculations and demonstrate its application to the case of some typical undulator field errors.

INTRODUCTION

Real undulators differ from ideal ones. The common way of the characterization of this difference is comparison of calculated spectral intensities of their radiation in forward direction and trajectories (see, e. g., [1]). For good undulator the reduction of spectral intensity is small and the trajectory deviation is less than the radius of first Fresnel zone divided by 2π, $\sqrt{\lambda L}/(4\pi)$, where L is the undulator length, and λ is the radiation wavelength. These two conditions are independent. Indeed, let us consider an undulator with parallel shift of electron trajectory in the middle (see below). The reduction of the forward-direction spectral intensity can be fully compensated by proper phase shift of radiation from the second half of the undulator (for example, by proper longitudinal shift of the second half). In this case we return constructive interference of the radiation from the undulator halves. But, in other but forward directions the path difference differs and spectral intensity will remain less than an ideal one. Therefore the total (integrated by angles) spectral power of radiation in this example is reduced. In this paper we consider the use of the spectral density of emitted radiation (the total number of emitted photons with given energy) as a figure of merit for an undulator. We derive analytical formula for this spectrum suitable for doing efficient numerical calculations and demonstrate its application for simple examples.

*Work supported by Russian Science Foundation (project 14-12-00480).
#O.A.Shevchenkoe@inp.nsk.su

SPECTRUM FORMULA

Let electron with charge e and coordinate $\mathbf{r}_0$ moves at velocity $\mathbf{v} = d\mathbf{r}_0/dt$. The Fourier harmonics of the radiation vector potential is [2]

$$\mathbf{A}_\omega(\mathbf{r}) = e\frac{e^{ikr}}{cr}\int_{-\infty}^{\infty}\mathbf{v}(t)e^{i\omega t - i\mathbf{k}\mathbf{r}_0(t)}dt, \quad (1)$$

where $k = \omega/c$, $\mathbf{r} = \mathbf{n}r$, $\mathbf{k} = \mathbf{n}k$. The spectral intensity (energy, radiated to the solid angle do and frequency interval $d\omega/(2\pi)$) is

$$dE_\omega = \frac{ck^2}{2\pi}\left|\mathbf{n}\times\mathbf{A}_\omega\right|^2 r^2 do\frac{d\omega}{2\pi} = \frac{e^2k^2}{2\pi c}\int_{-\infty}^{\infty}\int_{-\infty}^{\infty}\left[\mathbf{v}(t_1)\cdot\mathbf{v}(t_2) - \mathbf{n}\cdot\mathbf{v}(t_1)\mathbf{n}\cdot\mathbf{v}(t_2)\right]\cdot e^{i\omega(t_1-t_2)-i\mathbf{k}\left[\mathbf{r}_0(t_1)-\mathbf{r}_0(t_2)\right]}dt_1dt_2do\frac{d\omega}{2\pi} \quad (2)$$

Integration over the angles gives the total energy, radiated to the frequency interval $d\omega/(2\pi)$, or the spectral power,

$$dW_\omega = \int_{4\pi} dE_\omega = 2\frac{e^2k^2}{c}\int_{-\infty}^{\infty}\int_{-\infty}^{\infty}e^{i\omega(t_1-t_2)}\left[\mathbf{v}(t_1)\cdot\mathbf{v}(t_2)\left\langle e^{-ik\mathbf{n}\left[\mathbf{r}_0(t_1)-\mathbf{r}_0(t_2)\right]}\right\rangle - v_p(t_1)v_q(t_2)\left\langle n_pn_qe^{-ik\mathbf{n}\left[\mathbf{r}_0(t_1)-\mathbf{r}_0(t_2)\right]}\right\rangle\right]dt_1dt_2\frac{d\omega}{2\pi}, \quad (3)$$

where

$$\left\langle e^{-i\mathbf{na}}\right\rangle = \frac{1}{4\pi}\int_{4\pi}e^{-i\mathbf{na}}do = \frac{1}{4\pi}\int_0^\pi e^{-ia\cos\theta}2\pi\sin\theta\, d\theta = \frac{\sin a}{a}, \quad (4)$$

$$\left\langle n_pn_qe^{-i\mathbf{na}}\right\rangle = \left(\frac{\sin a}{a^3} - \frac{\cos a}{a^2}\right)\delta_{pq} + \left(\frac{\sin a}{a} - 3\frac{\sin a}{a^3} + 3\frac{\cos a}{a^2}\right)\frac{a_pa_q}{a^2}, \quad (5)$$

and $\mathbf{a} = k\left[\mathbf{r}_0(t_1) - \mathbf{r}_0(t_2)\right]$.

Taking into account that

$$k^2\mathbf{n}\cdot\mathbf{v}(t_1)\,\mathbf{n}\cdot\mathbf{v}(t_2)\,e^{-i\mathbf{k}\left[\mathbf{r}_0(t_1)-\mathbf{r}_0(t_2)\right]}=\frac{d}{dt_1}\frac{d}{dt_2}e^{-i\mathbf{k}\left[\mathbf{r}_0(t_1)-\mathbf{r}_0(t_2)\right]}$$

and integrating Eq. 3 by parts one can also obtain

$$dW_\omega=\frac{2e^2k^2}{c}\int_{-\infty}^{\infty}\int_{-\infty}^{\infty}\left[\mathbf{v}(t_1)\cdot\mathbf{v}(t_2)-c^2\right]\left\langle e^{-ik\mathbf{n}\left[\mathbf{r}_0(t_1)-\mathbf{r}_0(t_2)\right]}\right\rangle e^{i\omega(t_1-t_2)}dt_1dt_2\frac{d\omega}{2\pi}. \quad (6)$$

Plugging Eqs. 4, 5 into Eqs. 3, 6 gives Eq. 7:

$$2\pi\frac{dW_\omega}{d\omega}=2\frac{e^2k^2}{c}\int_{-\infty}^{\infty}\int_{-\infty}^{\infty}\left[\mathbf{v}(t_1)\cdot\mathbf{v}(t_2)-c^2\right]\frac{\sin a}{a}e^{i\omega(t_1-t_2)}dt_1dt_2. \quad (7)$$

Since $v_z dt = dz$, in paraxial $|x_1 - x_2|$, $|y_1 - y_2| << |z_1 - z_2|$ and ultrarelativistic $\gamma >> 1$ approximation

$$ct_1-ct_2\approx z_1-z_2+\frac{z_1-z_2}{2\gamma^2}+\int_{z_2}^{z_1}\frac{x'^2+y'^2}{2}dz, \quad (8)$$

Eq. 7 can also be written as shown in Eq. 9:

$$\begin{aligned}2\pi\frac{dW_\omega}{d\omega}&=2\frac{e^2k^2}{c}\int_{-\infty}^{\infty}\int_{-\infty}^{\infty}\left[1+x_1'x_2'+y_1'y_2'-\frac{1}{\beta_{z1}\beta_{z2}}\right]\frac{\sin a}{a}\cos\left[\omega(t_1-t_2)\right]dz_1dz_2\approx\\ &\frac{e^2k}{2c}\int_{-\infty}^{\infty}\int_{-\infty}^{\infty}\frac{(x_1'-x_2')^2+(y_1'-y_2')^2}{s}\sin\frac{k}{2\gamma^2}\left[s+\gamma^2\int_{z-s/2}^{z+s/2}\left(x'^2+y'^2\right)dz'-\gamma^2\frac{(x_1-x_2)^2+(y_1-y_2)^2}{s}\right]dsdz+,\\ &\frac{e^2k}{\gamma^2c}\int_{-\infty}^{\infty}\left\{\int_{-\infty}^{\infty}\sin\frac{k}{2\gamma^2}\left[s+\gamma^2\int_{z-s/2}^{z+s/2}\left(x'^2+y'^2\right)dz'-\gamma^2\frac{(x_1-x_2)^2+(y_1-y_2)^2}{s}\right]\frac{ds}{s}-\frac{\pi}{2}\right\}dz\end{aligned} \quad (9)$$

where $s = z_1 - z_2$ and $z = (z_1 + z_2)/2$. This integral does not contain fast-oscillating terms and can be calculated numerically for any paraxial trajectory. Now we will demonstrate the use of Eq. 9 for the simplest case of helical undulator and for planar undulator with parallel shift of electron trajectory.

IDEAL HELICAL UNDULATOR

For an ideal helical undulator

$$x=\frac{K}{\gamma k_u}\cos k_u z,\quad y=\frac{K}{\gamma k_u}\sin k_u z \quad (10)$$

for $0 < z < L$. Then for long ($k_uL = 2\pi N >> 1$) undulator

$$\begin{aligned}2\pi\frac{dW_\omega}{d\omega}&\approx\frac{e^2kK^2L}{\gamma^2c}\int_{-\infty}^{\infty}\frac{1-\cos u}{u}\sin\left\{\frac{k}{2\gamma^2k_u}\left[u\left(1+K^2\right)-2K^2\frac{1-\cos u}{u}\right]\right\}du+\\ &\frac{e^2kL}{\gamma^2c}\left\{\int_{-\infty}^{\infty}\sin\left\{\frac{k}{2\gamma^2k_u}\left[u\left(1+K^2\right)-2K^2\frac{1-\cos u}{u}\right]\right\}\frac{du}{u}-\frac{\pi}{2}\right\}\end{aligned}. \quad (11)$$

For weak ($K << 1$) undulator integral in (11) can be taken easily, and one obtains well-known result [3]

$$2\pi\frac{dW_\omega}{d\omega}\approx\frac{\pi e^2kK^2L}{\gamma^2c}\left[1-2\frac{k}{2\gamma^2k_u}\left(1-\frac{k}{2\gamma^2k_u}\right)\right]\vartheta\left(2\gamma^2k_u-k\right), \quad (12)$$

where $\vartheta(x)$ is Heaviside step function, $\vartheta(x) = 1$ for $x \geq 0$, $\vartheta(x) = 0$ for $x < 0$.

UNDULATOR WITH PARALLEL SHIFT OF TRAJECTORY

Now we will compare the undulator with parallel shift of electron trajectory (see Fig. 1) with an ideal one.

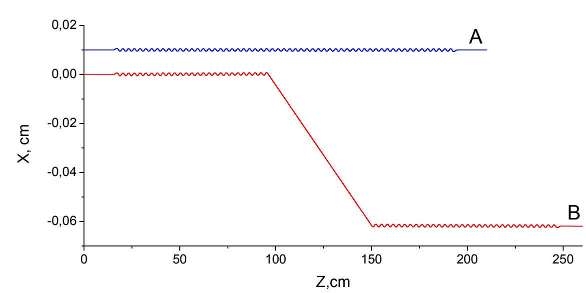

Figure 1: Calculated trajectories in ideal (A) and disturbed (B) undulators.

The calculated with Eq. 2 spectral intensities of forward-direction radiation (Fig. 2) at the frequency of interest are the same.

The corresponding total spectral powers, obtained with Eq. 9, are shown in Fig. 3.

ISBN 978-3-95450-133-5

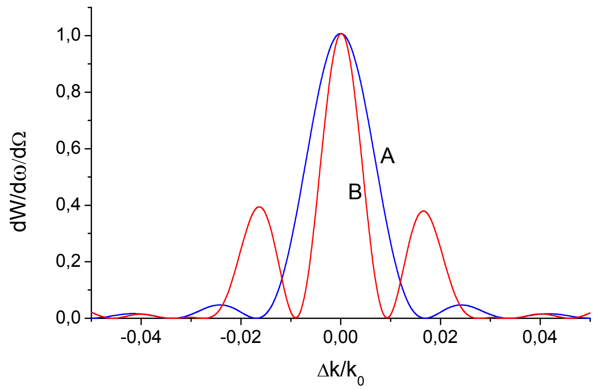

Figure 2: Spectral intensities of forward-direction radiation for ideal (A) and disturbed (B) undulators.

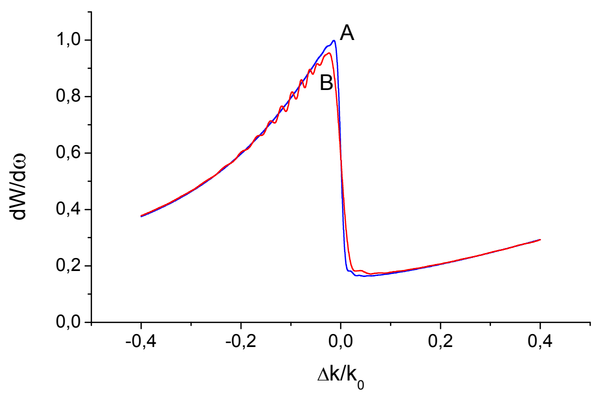

Figure 3: Total spectral powers for ideal (A) and disturbed (B) undulators.

CONCLUSION

In this paper we have shown, that the total spectral power of undulator radiation can be used to characterize the undulator quality. This quantity is less sensitive to the most of field disturbance than the forward-direction spectral intensitiy. On the other hand, in contrary to the forward-direction spectral intensitiy it is sensitive to all kinds of imperfections. Therefore instead of two figures of merit (forward-direction spectral intensitiy and trajectory straightness) one can optimize one only. Moreover, the corresponding variational problem for undulator field optimization can be considered.

ACKNOWLEDGMENT

This work is supported by Russian Science Foundation (project 14-12-00480).

REFERENCES

[1] E. Levichev and N. Vinokurov, Rev. Accel. Sci. Technol. **3**, 203-220 (2010).
[2] L.D. Landau and E.M. Lifshitz, *The Classical Theory of Fields*, Oxford, New York, Toronto, Sidney, Braunschweig: Pergamon Press, 1971, 172.
[3] J.D. Jackson *Classical Electrodynamics, 3rd Edition,* John Wiley & Sons, Inc., 1999, 690.

ISBN 978-3-95450-133-5